An isomerization reaction of a cyanine dye in n-alcohols: Microscopic friction and an excited-state barrier crossing

ARTICLE *in* THE JOURNAL OF PHYSICAL CHEMISTRY · OCTOBER 1991

Impact Factor: 2.78 · DOI: 10.1021/j100175a016

4 AUTHORS, INCLUDING:

Jouko korppi-tommola
University of Jyväskylä
127 PUBLICATIONS **2,603** CITATIONS

SEE PROFILE

largest cross sections. Since there are fewer acceptor states at 8.3 eV, there are more molecules with quenching cross sections <30 Å^2 for Xe($^3P_2$). Highly fluorinated molecules especially have small cross sections because there are few acceptor states. The correlation between $\sigma_Q(T)$ and the C_6 coefficient can be used to estimate the thermal quenching cross sections by molecules for Ar($^3P_0$), Ar($^3P_2$), and Xe($^3P_2$) atoms that have not been measured. The reactions of Ar($^3P_{0,2}$) with $SiCl_4$ and $SiCl_3H$ give a high branching fraction for $SiCl_2(\tilde{a})$.

Acknowledgment. This work was supported by the National Science Foundation, Grant 8822060. We also thank Dr. Paul Marcoux (Hewlett Packard Corp.) for a gift of vacuum equipment, which made this work possible.

An Isomerization Reaction of a Cyanine Dye in *n*-Alcohols: Microscopic Friction and an Excited-State Barrier Crossing

Jouko E. I. Korppi-Tommola,* Aulis Hakkarainen, Terttu Hukka,

Department of Chemistry, University of Jyväskylä, SF-40100 Jyväskylä, Finland

and Juhan Subbi

Institute of Chemical Physics and Biophysics, Estonian Academy of Sciences, Lenini Puistee 10, Tallinn 200001, USSR *(Received: July 10, 1990; In Final Form: June 5, 1991)*

The isomerization reaction of a cyanine dye, *N,N'*-diethyl-3,3'-tetramethylindocarbocyanine iodide (DiIC(2)), in eight *n*-alcohols at several temperatures was studied by using fluorescence lifetime measurements. In solutions from methanol to hexanol, hydrodynamic viscosity and a constant barrier seems to control the reaction. In long-chain solvents the constant-viscosity plots ($n > 4$) show nonlinear behavior, which becomes more apparent at high temperatures and low viscosities. The results suggest that when the size of the surrounding solvent molecule approaches the size of the isomerizing group the concept of hydrodynamic friction breaks down. Rotational molecular friction model for the reaction shows linear and solvent dependent η/T dependencies of the nonradiative lifetimes. Correcting for the relative volumes of the solvent and the solute allows fitting of all the observed reduced rates by using a constant barrier of isomerization. The diffusion limit of Kramer's theory and a nonlinear boundary condition was used to account for the rates observed at high values of friction. It seems that non-Kramers' behavior at high viscosities is related to frequency-dependent frictional effects, which become important when solvent motion as compared to the reaction rate becomes slow.

Introduction

Isomerization reactions are assumed to be responsible for the nonradiative decays observed for many dye molecules in solution subjected to laser excitation. Usually isomerization is taken as a single-coordinate minimum energy path, where coupling to a large-amplitude vibrational motion of a molecule or a molecular ion results in a solvent-controlled, temperature- and pressure-dependent nonradiative decay from the excited electronic state. The isomerization reaction may be controlled by zero or even apparently negative barriers. In many cases medium- or high-barrier behavior is observed.

Besides barrier height, solvent properties play an important role in determining the nonradiative isomerizing rate. For homologous series of solvents, e.g., *n*-alkanes,[1-5] in *n*-alcohols,[6-11] and in aliphatic nitriles[12,13] various theories have been used to predict the effect of the solvent on the nonradiative rate. Comparison has less frequently been made of the kinetics of a particular reaction in solvents with differing properties, e.g., in *n*-alcohols on one hand and polar solvents such as acetone and chloroform, etc., on the other.[10,13,14] Solvent viscosity may play an important role in *n*-alcohol solutions, while the dielectric constant of the medium may be important in polar non-hydrogen-bonding solvents. Rate constants for the same reaction may differ by a factor of 10 for solutions with identical bulk viscosities.[15] So far no existing theory can account for these highly solvent-dependent kinetic effects.

Studies of reactions in collision-free environment, i.e., in supersonic noble-gas expansions, are informative on the intramolecular relaxation channels of isomerization.[16-18] For the same

(1) Waldeck, D. H.; Lotshaw, T.; McDonald, B.; Fleming, G. R. *Chem. Phys. Lett.* **1982**, *88*, 297.
(2) Rothenberg, G.; Neugus, D. K.; Hochstrasser, R. M. *J. Chem. Phys.* **1983**, *79*, 5360.
(3) Sundström, V.; Gillbro, T. *Ber. Bunsen-Ges. Phys. Chem.* **1985**, *89*, 222.
(4) Lee, M.; Bain, P. J.; Han, C. H.; Haseltine, J. N.; Smith III, A. B.; Hochstrasser, R. M. *J. Chem. Phys.* **1986**, *85*, 4341.
(5) Hirata, Y.; Mataga, N.; Mukai, Y.; Koyama, Y. *J. Phys. Chem.* **1987**, *91*, 5238.
(6) Ippen, E. P.; Shank, C. V.; Bergman, A. *Chem. Phys. Lett.* **1976**, *38*, 76.
(7) Velsko, S. P.; Waldeck, D. H.; Fleming, G. R. *J. Chem. Phys.* **1983**, *78*, 249.
(8) Rentsch, S. K.; Gadonas, R. A.; Piskarskas, A. *Chem. Phys. Lett.* **1984**, *104*, 235.
(9) Sundström, V.; Gillbro, T. *Chem. Phys. Lett.* **1984**, *110*, 303.
(10) Ben-Amotz, D.; Harris, C. B. *Chem. Phys. Lett.* **1985**, *119*, 305; *J. Chem. Phys.* **1987**, *86*, 4856.
(11) Mokhtari, A.; Fini, L.; Chesnoy, J. *J. Chem. Phys.* **1987**, *87*, 3429.
(12) Hicks, J.; Vandersall, M.; Babarogic, Z.; Eisenthal, K. B. *Chem. Phys. Lett.* **1985**, *116*, 18.
(13) Hicks, J. M.; Vandersall, M. T.; Sitzmann, E. V.; Eisenthal, K. B. *Chem. Phys. Lett.* **1987**, *135*, 413.
(14) Martin, M. M.; Breheret, E.; Meyer, Y. H. *Chem. Phys.* **1989**, *130*, 279.
(15) Korppi-Tommola, J., to be published.
(16) Felker, P. M.; Syage, J. A.; Lambert, Wm. R.; Zewail, A. H. *Chem. Phys. Lett.* **1982**, *92*, 1.
(17) Syage, J. A.; Felker, P. M.; Zewail, A. H. *J. Chem. Phys.* **1984**, *81*, 4685; *J. Chem. Phys.* **1984**, *81*, 4706.

0022-3654/91/2095-8482$02.50/0

isomerization reaction the barrier height generally seems to be higher in a vacuum than in solution, suggesting that solvent molecules stabilize the reacting species and make crossing to the product side easier. Adding solvents to carrier gas in a jet experiment in a controlled manner[19] seems to be a promising way to study isomerization reactions in very small solvent–solute clusters and to get information of the solvent role during the isomerization reaction.

Use of macroscopic viscosity to describe the kinetics of reactions occurring at rates comparable to molecular collision rates is a dubious practice. Hydrodynamic viscosity is often related to the friction of the reaction via the Stokes–Einstein equation. Two boundary conditions are frequently used: the slip and the stick boundary conditions. It has been suggested that rotational friction could serve as a good measure of the microviscosity experienced by the isomerizing group in solution. Slip hydrodynamics often describes rotational friction of a molecule in solution adequately. In some cases subslip kinetics are observed.[22] Rotational friction can be obtained by measuring reorientational times of the solute and using the Hubbard relation.[7,21,22] Total friction of a reaction is the sum of the rotational and translational friction. In many cases it is not known which of them dominates and which hydrodynamics is applicable. This is reflected in the literature: in some cases using experimental rotational friction instead of hydrodynamic friction produces better agreement with the applied theories,[2,4,21] while in other cases no improvement has been observed.[7,23,24]

The theory of the dynamics of activated rate processes has experienced a revival[26–38,39,40] about 40 years after the appearance of Kramers' classical work "Brownian motion in the field of force and the diffusion model of chemical reaction".[38] The renewed interest is mainly a consequence of the accumulation in recent years of picosecond kinetic data on the reaction dynamics in solution. In some cases Kramers' theory seems to work[45] and in some cases it breaks down.[4,7,21,35] In many cases Kramers' theory predicts too slow kinetics at high values of friction. Various "corrections" have been suggested to preserve Kramers' behavior in cases where the theory fails. These include correcting for temperature- or medium-dependent barrier height,[12,13,24,45] using rotational friction to describe friction of the isomerizing reaction,[4,21]

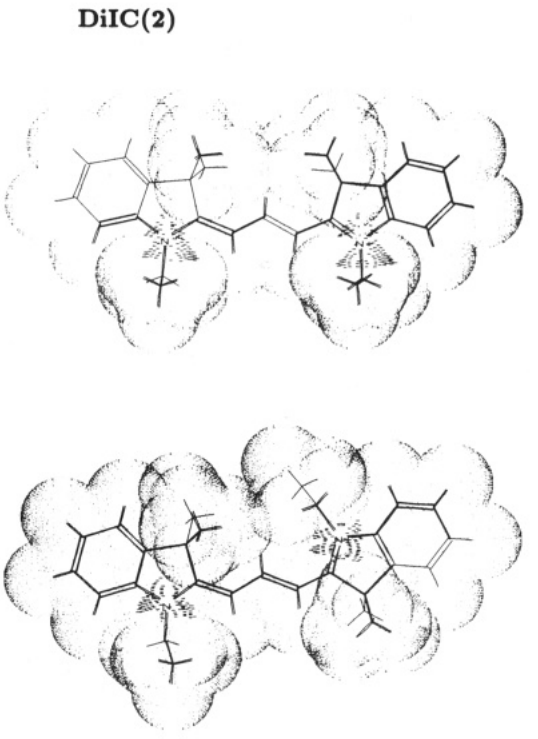

Figure 1. Cis (top) and trans (bottom) comformers of DiIC(2).

and estimating frequency depency of friction by using experimental parameters.[2,7,27]

A theory based on statistical free volume available in the liquid has been used to describe the fluidity of liquids.[39,40] This simple theory predicts a power-law dependence for the reduced isomerization rate as a function of viscosity as $k_{red} = D/\eta^{\alpha}$, provided that the constants D and α do not vary much from solvent to solvent.[7] The power law equation has been used to describe isomerizing and reorientational systems with amzingly good success.[7,21,27] Klassical kinetic model including parameters for average collision frequency and relative size of the solvent and solute has been used to develop equations describing the relaxation rate.[31] Questions have been raised concerning the multidimensionality of the isomerization coordinate and the dynamic coupling of the reacting species to the solvent environment along the reaction path.[24,25]

Nonradiative rate constants, hydrodynamic viscosity, and temperature are the physical observables used in the study of frictional effects on reaction dynamics. For the fast reactions under study, however, the concept of hydrodynamic friction often breaks down and the friction controlling the isomerization reaction may become dependent on time. This is particularly the case for high barrier reactions at low viscosities.[7] By including non-Markovian effects in the time-dependent friction term of the generalized Langevin equation and using the probability distribution from the generalized Fokker–Planck equation, Grote and Hynes obtained an apparently simple expression for the isomerization rate constant $k = k^{TST}(\lambda_r/\omega_b)$.[32] The practical problem in using this equation is that λ_r is given by a self-consistency relation, which includes a function describing the time dependence of friction of the system under study. Analytical expressions for such functions are not known. Bagchi and Oxtoby[27] have made an effort to derive such an expression from the Zwanzig and Bixon[41] equation for frequency-dependent translational friction and the Berne and Montgomery[42] equation for frequency-dependent rotational friction. They used a multitude of estimated and experimental parameters to numerically generate λ_r values at various shear viscosities.[27] Though their absolute values were strongly dependent on barrier frequency, the qualitative features of non-Kramers' behavior could be nicely produced.

In the present case we report results on an excited state isomerizing reaction of *N*,*N*′-diethyl-3,3′-tetramethylindocarbocyanine iodide (DiIC(2)) in *n*-alcohols. A one-dimensional reaction co-

(18) Felker, P.; Zewail, A. H. *J. Phys. Chem.* **1985**, *81*, 4706.
(19) Gibson, E. M.; Jones, A. C.; Phillips, D. *Chem. Phys. Lett.* **1987**, *136*, 454.
(20) Warren, J. A.; Bernstein, E. R. *J. Chem. Phys.* **1988**, *88*, 871.
(21) Lee, M.; Haseltine, J. N.; Smith III, A. B.; Hochstrasser, R. M. *J. Am. Chem. Soc.* **1989**, *111*, 5044.
(22) Ben-Amotz, D.; Scott, T. W. *J. Chem. Phys.* **1987**, *87*, 3739.
(23) Waldeck, D. H.; Fleming, G. R. *J. Chem. Phys.* **1981**, *85*, 2614.
(24) Bowman, R. M.; Eisenthal, K. B. *Chem. Phys. Lett.* **1989**, *155*, 99.
(25) Zhu, S.-B.; Robinson, G. W. *Chem. Phys. Lett.* **1988**, *153*, 539.
(26) Oster, G.; Nishijima, Y. *J. Am. Chem. Soc.* **1956**, *78*, 1581. Förster, Th.; Hoffmann, G. *Z. Phys. Chim. (Munich)* **1971**, *75*, 63.
(27) Bachi, B.; Oxtoby, D. W. *J. Chem. Phys.*, **1983**, *78*, 2735; Bagchi, B.; Fleming, G. R.; Oxtoby, D. W. *J. Chem. Phys.* **1983**, *78*, 7375.
(28) Bagchi, B.; Singer, A.; Oxtoby, D. W. *Chem. Phys. Lett.* **1983**, *99*, 225.
(29) Bagchi, B. *Chem. Phys. Lett.* **1985**, *115*, 209.
(30) Bagchi, B. *Chem. Phys. Lett.* **1987**, *135*, 558.
(31) Skinner, J. L.; Wolynes, P. G. *J. Chem. Phys.* **1978**, *69*, 2143. Skinner, J. L.; Wolynes, P. G. *J. Chem. Phys.* **1980**, *72*, 4913.
(32) Grote, R. F.; Hynes, J. T. *J. Chem. Phys.* **1980**, *73*, 2715.
(33) Pollak, E. *J. Chem. Phys.* **1986**, *85*, 865.
(34) Cartling, B. *J. Chem. Phys.* **1987**, *87*, 2638.
(35) Lee, J.; Zhu, S.-B.; Robinson, G. W. *J. Phys. Chem.* **1987**, *91*, 4273.
(36) Lee, S.; Karplus, M. *J. Phys. Chem.* **1988**, *92*, 1075.
(37) Sparpaglione, M.; Mukamel, S. *J. Phys. Chem.* **1987**, *91*, 3938; *J. Chem. Phys.* **1987**, *88*, 3263; *J. Chem. Phys.* **1987**, *88*, 4300.
(38) Kramers, H. A. *Physica* **1940**, *7*, 284.
(39) Doolittle, A. K. *J. Phys. Chem.* **1951**, *22*, 1471.
(40) Cohen, M. H.; Turnbull, D. *J. Chem. Phys.* **1959**, *31*, 1164.
(41) Zwanzig, R.; Bixon, M. *Phys. Rew A* **1970**, *2*, 2005.
(42) Montgomery, J. A.; Berne, B. J. *J. Chem. Phys.* **1977**, *66*, 2770.
(43) Onuchic, J. N.; Wolynes, P. G. *J. Phys. Chem.*, **1988**, *92*, 6495.
(44) Keery, M., Fleming, R. *Chem. Phys. Lett.* **1982**, *93*, 322.
(45) Åkesson, E.; Sundström, V.; Gillbro, T. *Chem. Phys. Lett.* **1985**, *121*, 513; *Chem. Phys.* **1986**, *106*, 269; Åkesson, E. Ph.D. Thesis, Umeå Universitet, **1989**.

ordinate is assumed. According to our MMX calculations (PCMODEL, Serena Software) the minimum-energy reaction coordinate of the ground electronic state is the rotation around the carbon–carbon bond closest to the charged nitrogen (Figure 1). The minimum-energy conformer is that with the ethyl groups of the dye in a cis position with respect to each other. The minimum energy rotation proceeds from cis to trans and requires over 200 kJ mol^{-1} of energy in the ground state. The energy of the trans form is about 7 kJ mol^{-1} higher than that of the cis conformer. Rotations around the center bonds are heavily restricted by steric hindrance. Though our calculations are valid for the ground state, it seems fair to assume that isomerization in the excited electronic state also proceeds along the same coordinate but needs less energy.

According to our results the excited-state isomerization reaction proceeds roughly according to the hydrodynamic model of friction and under a constant barrier in solutions from methanol to hexanol. The isoviscosity plots give almost parallel lines in these solutions independent of viscosity. Nonlinear behavior is observed for long-chain alcohols, with the nonlinearity becoming more apparent at high temperatures. This has been considered as an indication of temperature-dependent barrier height in recent absorption recovery and fluorescence quantum yield studies of DiIC(2).[45]

We have used three alternative approaches to interpret our results. First we used an experimentally observed relation between the barrier height and hydrodynamic viscosity to correct for the deviations from non-Kramers' behavior in the nonlinear region of the isoviscosity plots. The approach allowed for excellent Kramers' fit of the observed rates; however, unreasonable Kramers' parameters were obtained. We then used a rotational relaxation model and plotted the nonradiative rates as a function of η/T. Solvent dependence of these plots suggested developing rotational correlation times including relative volume effects of the solute and solvent. Such a procedure brought the observed reduced rates nicely on a smooth curve. In the third approach we calculated "effective" frictions for each solvent by extrapolating the linear parts of the isoviscosity plots into the nonlinear region. This method gave correlations between the hydrodynamic viscosity and "effective" friction in each solvent. Using "effective" values of friction and a constant barrier, all data points could be fitted to Kramers' equation, with slight but obvious underestimation of rates at high viscosities.

To study non-Kramers' behavior at high values of friction, we assumed that the reduced rates follow the inverse law of molecular friction (the Smoluchowski limit).[32,43] For friction we assume a power-law type boundary condition. Using these concepts, we derive analytical equations for temperature and isoviscosity dependencies of the nonradiative rates. It seems that our approach allows for better description of the reduced rates at high values of friction than is obtained by using volume corrected friction and Kramers' equation.

Experimental Section

Absorption spectra of DiIC(2) dye in various solutions were recorded on a Perkin-Elmer Lamda5 visible–UV spectrometer interfaced to an IBM/AT personal computer. Home-written scan and graphics programs were used to record and store the spectral data. Fluorescence spectra were recorded with an excimer laser pumped (ELIM5,Tallinn) dye laser (VL-10,Tarto) and a 25-cm monochromator equipped with a gated OMA III-detection system and a 1460 data processor (EG&G, PAR). The intensities were calibrated against light-bulb radiation assuming Planck's intensity distribution.

A synchronously pumped, mode-locked and cavity-dumped dye laser (Coherent Inc., argon ion laser INNOVA 15W, dye laser 599-04, mode locker 467, cavity dumper 7200) was used to produce light pulses of 8-ps duration. The cavity dumper was moved away from the dye laser to allow for broader tunability and almost twice the output power as compared with the folded cavity configuration provided by the manufacturer. In our configuration the average output of the laser is typically 50 mW at 4-MHz repetition rate for the Rhodamine 110 dye used in the present study. A home-built autocorrelator, operated through the C-language program PICO 6.0 on a IBM/AT compatible computer, was used to monitor the pulse profiles. The program controls a stepper motor of an optical delay line at 10-kHz pulsing rate, collects data points from a lock-in amplifier and writes finally 1024 16-bit data points for each scan on a floppy disk. The signal can be examined on the computer screen immediately after measurement. Total scan time is a few minutes. The autocorrelator can used to record absorption recovery times up to 6 ns in the present configuration.

Time-correlated single-photon counting was used to monitor fluorescence decays. The start signal was taken from a 500-ps rise time photodiode (RCA, C30902E), and the stop signal from a Hamamatsu R1654U-07 microchannel plate photomultiplier. Both signals were then led to constant fraction discriminators (CFD, Ortec 583). Timing pulses of the single photon events were directed to a time-to-analog converter (Ortec467) and sorted on a multichannel analyzer (Nokia LP4700). Data were then transferred via a personal computer (IBM/AT) to a VAX 8650 mainframe computer for deconvolution analysis. The program FLUORRES, originally written in Riso, Denmark, after modification for our own needs, was used to deconvolute the fluorescence lifetimes from the recorded decay signals. The program can handle up to five Gaussian components of the instrument function and up to five exponentials. Deconvolution analysis was performed for a set of 1024 points of each decay curve. The variance of the fit was generally between one and two for signals having 50 000 counts in the maximum channel. In the present experiments the instrumental response function, which was measured by scattering laser light from the rough back surface of a mirror, was typically 80 ps.

The samples were kept in a spinning (1200 rpm) cell made of stainless steel frame, 100-mm quartz windows, and Teflon O-rings. The laser path length in the cell was about 3 mm. The exciting beam entered the cell at a 45° angle, and the fluorescence was collected at 90° with respect to the incoming beam. Spinning the sample reduces local heating of the laser as well as scatter from microscopic particles in solution. Accumulation of signal from possible long-lived species in solution can also be reduced by having a fresh excitation volume for each exciting laser pulse. We collected decay histograms normally at 400-kHz repetition rate of the laser giving roughly 10 pulses/excitation volume. Excitation at 8 kHz, when every fifth excitation volume receives a single laser pulse, gave identical kinetics. Signals were collected at a counting rate of about 2% of the repetition rate of the laser up to 50 000 counts at the peak of each signal. This corresponds to total of over a million coincidences for each decay. Magic angle detection geometry was used. Cutoff filters were used to remove the exciting light from the fluorescence signals. The start signal was taken from the photodiode. The spinning cell was cooled or heated by passing nitrogen vapor or hot air through the cell. Temperatures were measured from the inside wall of the cell by using a thermistor. Thermistor readings were calibrated by freezing known solvents in the cell. Temperatures are believed to be correct to within 2 °C. The lowest temperature obtained so far is roughly −130 °C (the cell is not evacuated).

The cyanine dye was purchased from Molecular Probes Inc. (Texas). The solvents normally used were of high spectral purity grade available from Merck Co. Some of the long-chain solvents were carefully distilled before use. Solvent emission signals were checked before making experiments in solution.

Results and Discussion

Absorption recovery lifetimes and fluorescence quantum yields of DiIC(2) in *n*-alcohol solutions have been reported recently,[45] along with data for the chemically similar but larger dye molecules DiI(6) and DiIC(14). In the present study we report fluorescence lifetime measurements for the DiIC(2) dye in *n*-alcohols. The lifetimes have been measured at viscosities from 1 to 300 cP and at temperatures from 80 to −100 °C.

The DiIC(2) dye has a long-lived photoisomer[46] absorbing at about 570 nm. To study emission from this possible isomer in solution, fluorescence spectra were recorded at several excitations

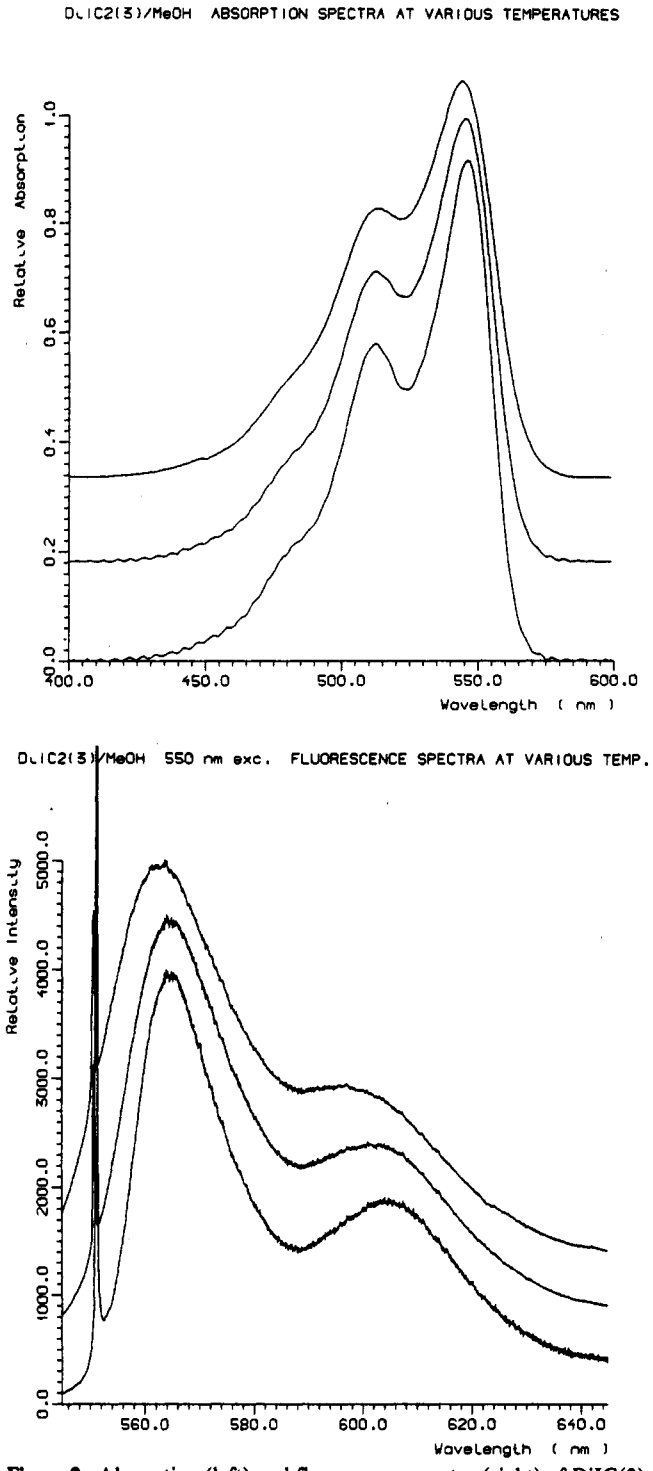

Figure 2. Absorption (left) and fluorescence spectra (right) of DiIC(2) in methanol at various temperatures. The temperatures from top to bottom 25, −20, and −60 °C, respectively, in both spectra. The sharp peak at 550 nm in the fluorescence spectra is the unfiltered exciting laser line.

over the absorption band using an excimer laser pumped dye laser as the exciting source. No emission could be assigned to the photoisomer, not even at high intensities of excitation. Since picosecond pulses are several orders of magnitude lower in intensity, it is unlikely that photoisomer was excited during the kinetic measurements. We also checked for cumulative effects by collecting data at very low repetition rates of the laser (8 kHz), but no difference in the kinetics was observed as compared to results obtained at higher repetition rates. Steady-state absorption and fluorescence spectra were recorded at several temperatures (Figure 2). Two changes are apparent in the spectra: absorption and emission line widths become narrower and the peak maxima are red-shifted as temperature decreases, the fluorescence shift

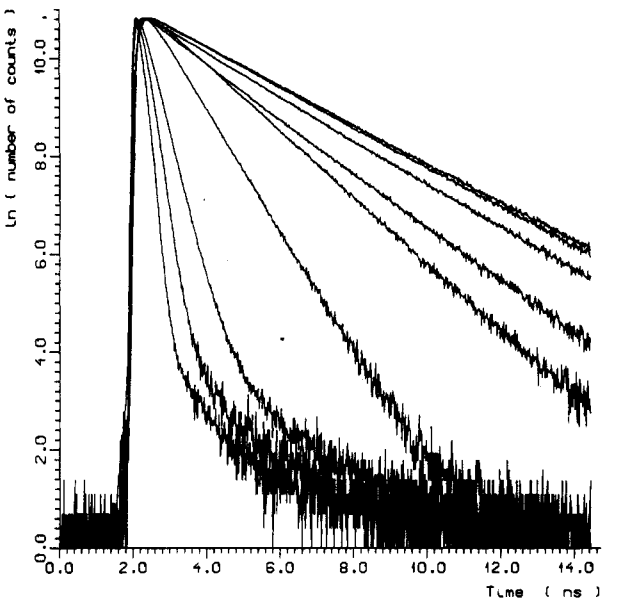

Figure 3. Fluorescence decay curves of DiIC(2) in ethanol solution at temperatures 43, 21, −35, −59, −75, −97, −119 and −134 °C. Long lifetimes are observed at low temperatures. The S/N ratio was better than 10000:1.

TABLE I: Least-Squares Parameters of the Arrhenius Plots of the DiIC(2) Kinetics in *n*-Alkanols[a]

solvent	A	B	temp range, °C	E_a, kJ mol^{-1}	E_η, kJ mol^{-1}
MeOH	−1.82	29.1	+25 to −90	15.1 (1.3)	7.6
EtOH	−2.00	29.1	+50 to −90	16.7 (0.2)	9.2
PrOH	−2.52	30.6	+50 to −80	21.0 (0.3)	13.5
BuOH	−2.71	30.9	+60 to −60	22.6 (0.2)	15.1
HexOH	−2.80	30.8	+70 to −40	23.3 (0.8)	15.8
OctOH	−3.15	31.6	+80 to −20	26.2 (0.4)	18.7
DecOH	−3.52	32.6	+50 to +0	29.2 (0.5)	21.7
DodeOH	−3.50	32.4	+80 to +25	29.1 (1.3)	21.6

[a] Radiative lifetime of 2.8 ns and the equation $\ln k_{nr} = A/T + B$ were used to get the parameters. A barrier height of $E_0 = 7.48$ kJ mol^{-1} was used to calculate E_η. Numbers given in parentheses are standard deviations.

becoming pronounced, about 10 nm.

The observed kinetics of the DiIC(2) dye seemed to be single exponential throughout the experiments. Fluorescence lifetimes were recorded at several temperatures in each solvent by using 550-nm excitation at maximum absorption of the dye. The radiative lifetime of 2.8 ns was used[45] to calculate isomerization rate constants k_{nr} via the relation $k_0 = \tau_0^{-1} = k_f + k_{nr}$, where k_f is the radiative rate constant and k_0 the observed rate constant. Some decay curves in ethanol solution at various temperatures are shown in Figure 3. Arrhenius plots of the kinetic results in all *n*-alcohols studied are shown in Figure 4, top. The least-squares parameters of the fits, and the temperature ranges are listed in Table I. The activation energies obtained from these plots contain a contribution from the barrier and from viscosity effects. Traditionally it has been assumed that $E_a = E_0 + E_\eta$, where E_0 is the barrier height and E_η the viscosity-induced part of the activation energy. By using kinetic data at constant viscosities, we can extract the barrier height (E_0) of the reaction. An exponential equation was fitted to the reported viscosities of each *n*-alcohol at various temperatures.[48,49] The least-squares parameters of these fits are given in Table II. Isoviscosity plots, covering a viscosity range from 1 to 16 cP and showing roughly two linear regions at each viscosity

(46) Deleted in proof.
(47) Kuzmin, V. A.; Darmanyan, A. P. *Chem. Phys. Lett.* **1978**, *54*, 159.
(48) Karapet'yants, M.Kh.; Yen, K.-S. *Izv.Vysshikh. Uchebn.Zavadenii, Khim. Khim. Tekhnol.* **1961**, *4*, 580.
(49) Landolt-Börnstein, *Zahlenwerte und Functionen*, Sechste Auflage, Band II, Teil 5; Springer-Verlag: Berlin, 1969; pp 208–230.

TABLE II: Least-Squares Parameters of Viscosities of *n*-Alkanols at Various Temperatures[a]

solvent	*A*	*B*	temp range, °C
MeOH	1278.4	−4.885	+65 to −90
EtOH	1567.7	−5.199	+75 to −100
PrOH	2109.8	−6.400	+60 to −80
BuOH	2306.0	−6.791	+110 to −50
HexOH	2584.6	−7.154	+150 to +5
OctOH	2995.3	−8.043	+90 to +15
DecOH	3173.5	−8.198	+90 to +20
DodecOH	3430.0	−8.695	+90 to +25

[a] The viscosities have been fitted to the equation $\ln \eta = A/T + B$, where temperature is given in absolute scale and viscosities η in centipoise. Experimental values for least-squares fits have been taken from refs 42 and 49.

are shown in Figure 4, bottom. Two important results can be seen: (1) for solutions from methanol to hexanol the barrier height E_0 = 7.5 kJ mol^{-1} is constant, independent of viscosity; (2) for solutions from hexanol to dodecanol the plots are linear but the slopes become steeper at low viscosities, corresponding to barrier heights of about 10 kJ mol^{-1} at 16 cP and 14 kJ mol^{-1} at 1 cP. In these latter solutions E_0 is apparently dependent on viscosity. Now the viscosity dependency of the barrier height at these viscosities can be adequately described by the equation

$$E_0(\eta) = E_{00} + A/\eta \qquad (1)$$

where E_{00} is the barrier height at infinite viscosity and A is constant. For solutions from butanol to dodecanol values of E_{00} = 10.5 kJ mol^{-1} and A = 3.47 kJ mol^{-1} cP were obtained.

What is then the origin of the apparent viscosity dependence of the barrier height? The absorption and fluorescence spectra of DiIC(2) have been shown to exhibit a red shift (about 7 nm) as one moves from methanol to hexanol solutions, while no further shift is observed in higher alcohols.[45] According to the present study, a constant barrier height is obtained for these solutions for a wide range of viscosities (Figure 4, bottom). Accordingly the excited-state potential surface is lowered with unchanged barrier height as one moves from methanol to hexanol solutions. In these solutions the fairly large dye molecule isomerizes in a bath of smaller, self-associated solvent molecules. Isomerization probably results in the breaking of hydrogen bonds of clustered solvent molecules, but these will rapidly relax to their original self-bonded structure once the reaction has taken place. Isomerization occurs in a fairly homogeneous environment. The assumptions of Brownian motion are valid, and the reaction is controlled by a constant barrier and one expects Kramers' hydrodynamic theory to work.

Barrier height generally seems to be larger in long-chain than in short-chain alcohols. Moreover, the barrier height appears to increase with temperature and with decreasing viscosity (see Figure 4, bottom). Spectroscopic results suggest that no further shift of the initial potential surface can be expected.[45] In these solutions then the potential well remains roughly at fixed position, while the barrier apparently becomes higher.

In these solutions the size of the isomerizing group of DiIC(2) becomes equal or smaller than that of the solvent molecule. The increasing size of the solvent molecule may have two effects on the reaction. On one hand, more energy is needed to open a solvent cage for the isomerization to take place. A bigger solvent molecule has to be removed away, and qualitatively this means higher barrier. On the other hand, the probability of a single collision to induce isomerization reaction increases due to mass effect. This probability is strongly dependent on the frictional conditions in the solution. According to our results the nonradiative rates become unexpectively high, especially at elevated temperatures. The true friction of the reaction in these solutions is smaller than that given by the hydrodynamic viscosity. This may be a result of two factors: first, the solute has more free space to isomerize in long-chain solvents than in smaller size solvents; second, the solute may feel slower response from the bulkier solvent environment during isomerization, i.e., the time scale of isomerization

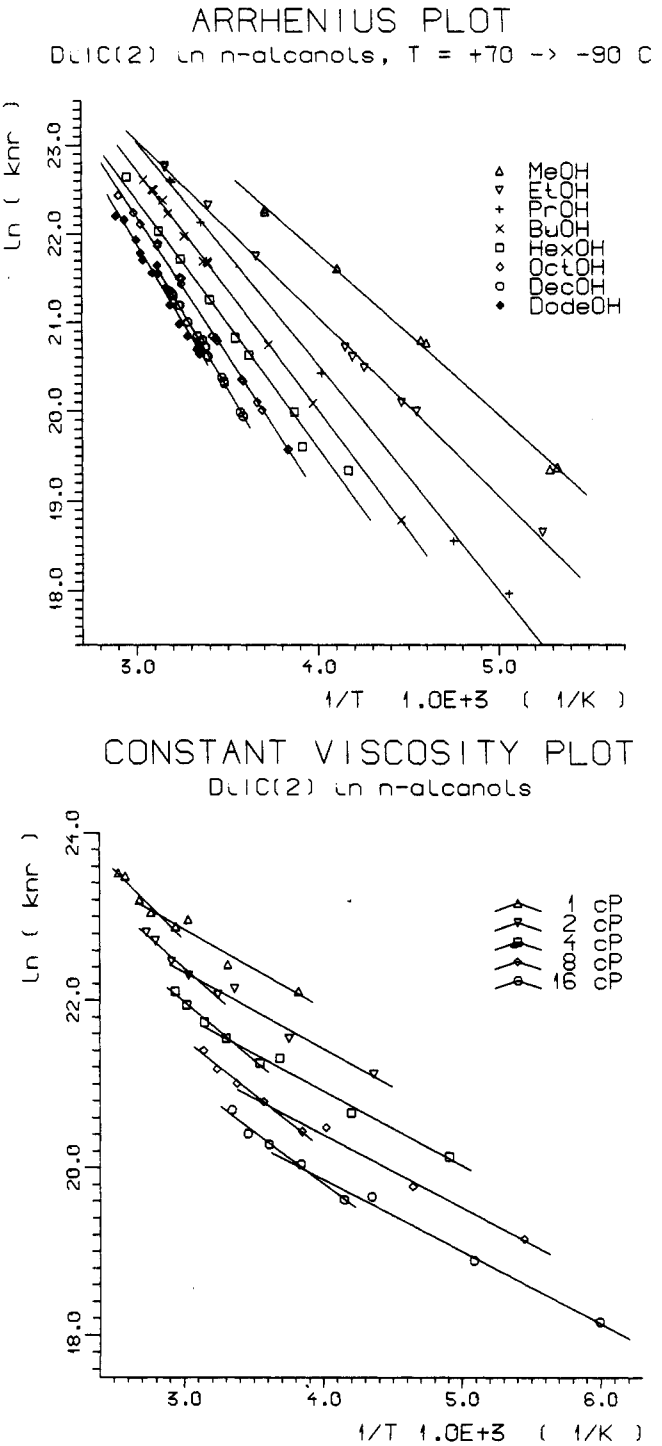

Figure 4. Top (a): Arrhenius plots of eight *n*-alcohol solutions of DiIC(2) (solvents from methanol to dodecanol). The lines represent least-square fits to the observed rates. Arrhenius parameters are given in Table I. Bottom (b): Isoviscosity plots of isomerization of DiIC(2). Viscosities used to produce the plots were calculated by using parameters given in Table II.

becomes fast as compared to the time scale of solvent response. The DiIC(2) dye is a nearly prolate symmetric top (Figure 1). The isomerizing takes place roughly around the long axis of the molecule. Isomerization feels rather rotational than translational friction in solution. This kind of motion may easily take place in a solvent cavity, and the frictional forces (even subslip[22]) of the reaction may become small.

Our measurements show that both absorption fluorescence spectra of DiIC(2) are red-shifted as the ethanol solution is cooled from 25 to about −60 °C. Isoviscosity plots suggest that higher viscosities and lower temperatures favor a slightly lower barrier. This can be interpreted as stabilizing of the excited state of the

TABLE III: Nonradiative Lifetimes of DiIC2 in n-Alkanol Solutions at Freezing Temperatures

solvent	freezing temp, T/°C	viscosity, η/cP	obsd lifetime, τ_0/ns
MeOH	-93.9	9.4	1.92
EtOH	-117.3	117	2.72
PrOH	-126.5	7170	2.79
BuOH	-89.5	318	2.73
HexOH	-46.7	70.6	2.19
OctOH	-16.7	39.2	1.62
DecOH	-7.0	22.8	1.18
DodecOH	+26.0	15.9	0.75

reacting species by the increasingly polar solvent environment at low temperatures. Results reported for isomerization reactions in vacuo and in solution suggest the same. In the case of stilbene, a higher barrier is observed for an isolated molecule in jet expansion experiments than for the same reaction in solution.[2,3,13,17,18] For DiIC(2) dye in various solvents there is no clear correlation between the dielectric constant of the solvent and the nonradiative rate.[45] However, a qualitatively fast rate correlates with high dielectric constant and low viscosity.

Freezing of the Isomerization Reaction at Phase Transition. Our experimental setup allows collecting fluorescence signals from a spinning sample cell even if the solution is frozen. The observed fluorescence lifetimes in all solvents seem to approach a value of 2.8 ns after freezing. Viscosities at freezing temperatures and the corresponding nonradiative rate constants are presented in Table III. In octanol, decanol, and dodecanol solutions at the freezing point, nonradiative rates are still much faster than the radiative lifetime. Cooling the solutions beyond freezing results in a sudden jump of the rate, the typical change of a first-order phase transition (Figure 5). This can be taken as evidence of hindering of the isomerization reaction at freezing of the solvent. After freezing, some nonradiative relaxation continues to occur, but at a considerably slower rate. The relaxation may take place through coupling of the electronic transition to lattice vibrations of the crystalline solvent. Smaller jumps are observed in hexanol and in methanol, a continuous change of the rate in ethanol, butanol, and propanol is observed. In the latter solvents viscosities at freezing temperatures are 197, 318, and 7170 cP, respectively, suggesting that isomerization is almost completely hindered even before freezing. The observations can be correlated to the types of phase transitions at freezing of the solvents concerned. It is known that long-chain alcohols crystallize more promptly than shorter alcohols that form glasses.

Kramers' Model of Viscosity-Dependent Barrier Crossing. Kramers' theory can be described as a particle trapped in a one-dimensional potential well, which is separated by a harmonic barrier E_0 from another, possibly deeper well. The particle is immersed in a medium, which on one hand exerts a frictional force on the particle and on the other hand gives it enough energy to escape the well. It is assumed that the motion of the particle can be described by the Langevin equation, which contains a normal kinetic term, a friction term, the force from the potential energy surface, and the external Gaussian random force term. At the low-viscosity limit the theory gives isomerizing rates proportional to friction:

$$k(\xi) = (\omega_0/2\pi)(\xi)e^{-E_0/kT} \quad (2)$$

where ω_0 is the harmonic frequency at the bottom of the well, ξ is the friction coefficient, and E_0 is the barrier height. In theories of Brownian motion friction is related to the velocity relaxation time of the reaction coordinate via $\tau_v = \mu/\xi$, where μ is the effective mass of the coordinate. In the low-viscosity limit the momentum relaxation time is very long compared to free motion time scales, i.e., the frictional forces are a small perturbation on the free motion. In the intermediate friction region Kramers showed that the escape rate is described by

$$k(\xi) = (\omega_0/2\pi)\{[(\xi/2\mu\omega_b)^2 + 1]^{1/2} - (\xi/2\mu\omega_b)\}e^{-E_0/kT} \quad (3)$$

where ω_b is the harmonic frequency at the top of the barrier. In

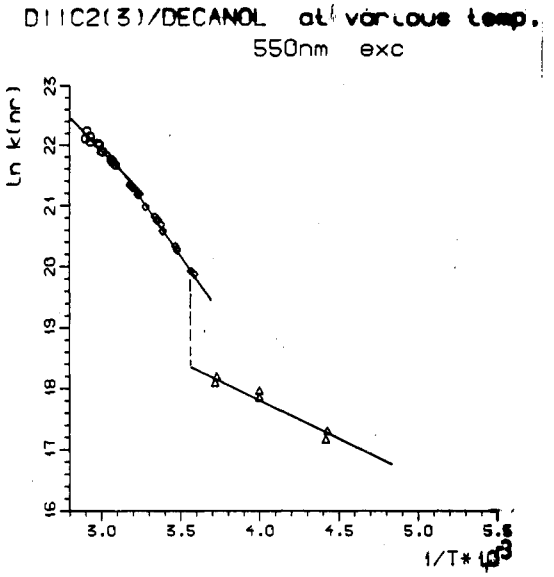

Figure 5. Arrhenius plot of the kinetics beyond freezing in n-decanol solution. A sudden jump occurs at the freezing point of the solvent (at abouut 26 °C), indicating hindering of the isomerization reaction in the solid state.

fitting eq 3 to the reaction rates of isomerization, hydrodynamic viscosity is often used to represent the friction coefficient. The high-viscosity limit of Kramers' theory predicts a $1/\xi$ dependence of the reduced rates.[32,38]

$$k(\xi) = (\omega_0\omega_b/2\pi)(1/\xi)e^{-E_0/kT} \quad (4)$$

At this limit friction is very large and velocity correlation time is short with the time scales of free motion. This limit is often called the Smoluchowski or the diffusion limit of Kramers' theory.

We have fitted our rate constants from methanol to hexanol solutions to Kramers' equation using hydrodynamic approximation of friction and the barrier height of 7.5 kJ mol^{-1}. The calculated curve slightly but clearly underestimates the reduced rates at high viscosities (Figure 6). Kramers' parameters $A = 2.1 \times 10^{11}$ 1/s and $B = 1.65$ cP give $\omega_0 = 44$ cm^{-1} and $\omega_b = 365$ cm^{-1} for the well and barrier wavenumbers, respectively. Structural parameters from ref 45 and the slip boundary condition were used to obtain the wavenumbers. Our MMX calculations for the ground state suggest a reaction coordinate where motion around the last carbon bond joining the carbon chain to the ring moiety containing the charged nitrogen serves as a minimum energy channel for the nonradiative decay (Figure 1). Typical frequencies of this kind of torsions range from 20 to 200 cm^{-1}. In the excited electronic state slightly smaller values are expected. The wavenumber obtained from Kramers' fit for the initial potential well falls in this region and supports the idea of a torsional mode to be responsible of the nonradiative decay in the excited state. From absorption recovery data value of 33 cm^{-1} was obtained for the well frequency of the same dye.[45]

The kinetics in hexanol through dodecanol behaves differently. We first used the average barrier height of 11.5 kJ mol^{-1} to produce a Kramers' fit. Much too low estimates of the reduced rates at high viscosities were obtained. To improve the fit, viscosity dependence of the barrier height was included in the calculation by using eqs 1 and 3 and the parameters $E_{00} = 10.5$ kJ mol^{-1} and $A = 3.5$ kJ mol^{-1} cP. The overall fit looks very good (Figure 7) and produces Kramers' constants $A = 4.1 \times 10^{13}$ 1/s and $B = 0.28$ cP. These correspond to wavenumbers of $\omega_0 = 1390$ cm^{-1} and $\omega_b = 63$ cm^{-1}. These wavenumbers do not suggest physically meaningful behavior. Vibrations having eigenfrequencies of the order of 1000 cm^{-1} or larger are not likely to be thermally populated. The frequency at the barrier top, ω_b, becomes smaller than the corresponding frequency in short-chain alcohols suggesting a shallow barrier. The isoviscosity plots of these solutions indicate opposite behavior. Accordingly, we conclude that the apparent dependence of the barrier height on viscosity actually is an in-

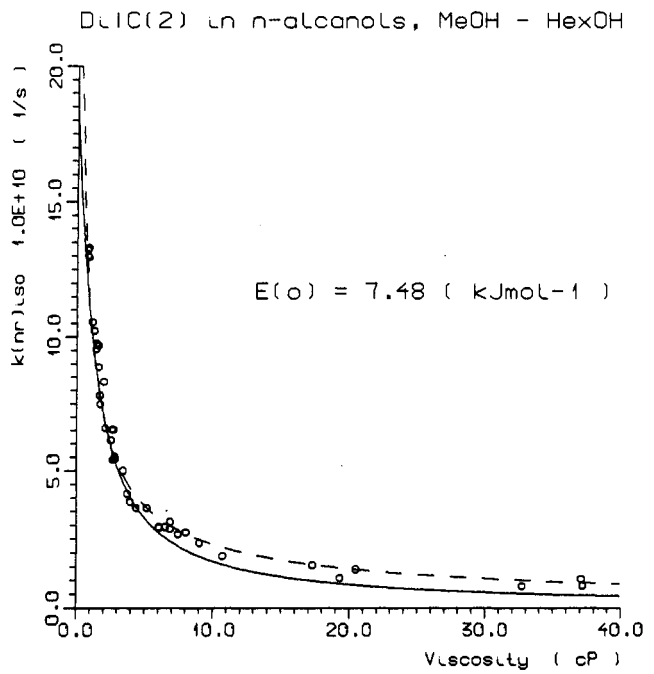

Figure 6. Fit of Kramers' equation (solid line) and the power law equation (dashed line) with the observed reduced rates. Kramers' parameters were $A = 2.10 \times 10^{11}$ 1/s and $B = 1.65$. Power law parameters were $D = 1.17 \times 10^{11}$ 1/s and $\alpha = 0.70$. Results from methanol through hexanol solutions and a constant barrier height of 7.5 kJ mol^{-1} were used.

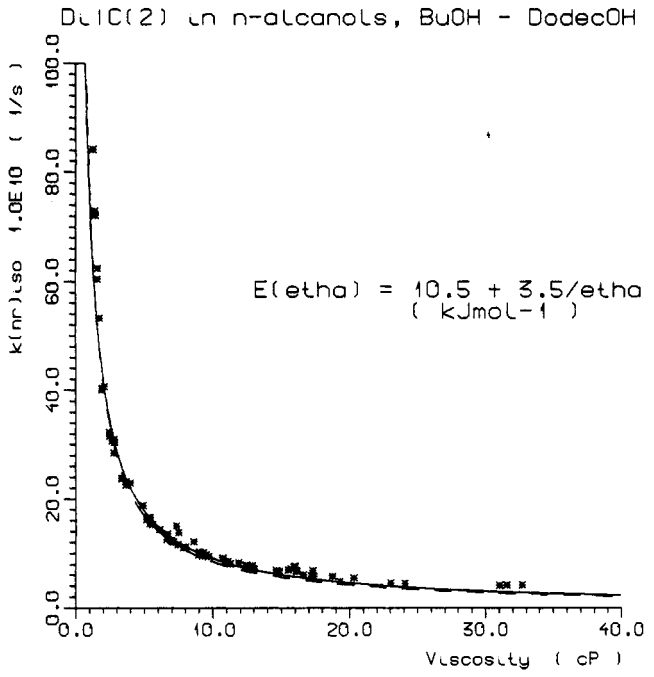

Figure 7. Fit of Kramers' equation (solid line) and the power law equation (dashed line) with the reduced rates using "viscosity-dependent barrier height", eq 1. Kramers' parameters are $A = 4.1 \times 10^{13}$ 1/s and $B = 0.28$. Power law parameters are $D = 8.72 \times 10^{11}$ 1/s and $\alpha = 1.01$.

dication of changing frictional conditions of the isomerization reaction. In these solutions the relative size of the solute molecule becomes equal to or smaller than that of the solvent molecule. Under these conditions, i.e., classical Stokes–Einstein model for rotational motion in solution brakes down and nonhydrodynamic behavior of kinetics may be expected provided that rotational friction controls the reaction.

The isomerization reaction of the DiIC(2) molecule does not change the shape of the molecule extensively (Figure 1). Isomerization takes place roughly around the long axis of the molecule. It seems fair to assume that rotational motion probes the fiction of the isomerization reaction of the nearly prolate molecule quite well. According to Dote, et al.[50] rotational correlation time is

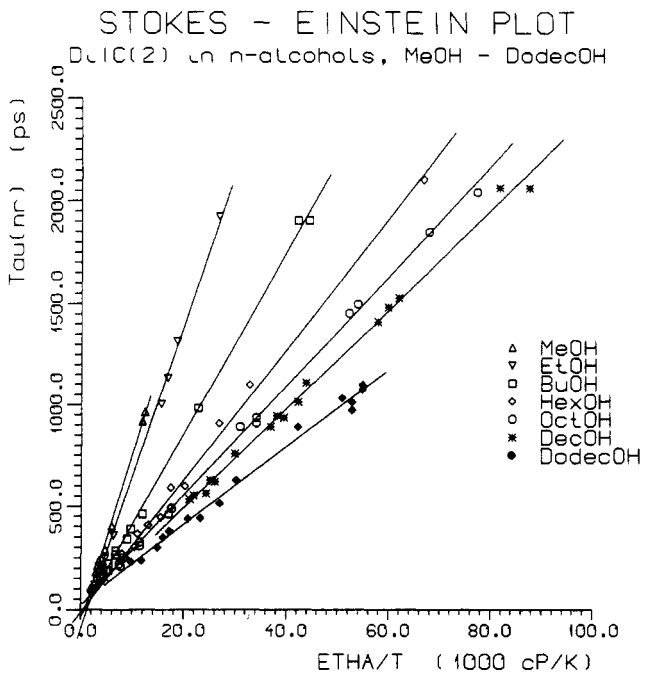

Figure 8. Least-square fits of Stokes–Einstein equation with the nonradiative lifetimes in various *n*-alcohol solutions.

related to viscosity, temperature, the proper boundary condition, and relative volumes of the solute and solvent molecules, respectively. Theory accounts for the decreased solute–solvent contact with decreasing ratio of the solute/solvent size. The theory has a drawback of not being able to account for faster rotational correlation times observed in *n*-alcohols as compared to hydrocarbon solutions of the same viscosity for the same solute. A simple model for microscopic rotational friction has been proposed by Gierer and Wirtz (G–W).[51] In their layered shell model the friction coefficient becomes smaller with decreasing solute–solvent volume ratio. For very small solvent molecules in solution G–W theory predicts Stokes–Einstein result for stick boundary condition and for very large solvent molecules the hydrodynamic slip boundary condition is obtained.

We have made both DKS and G–W corrections for three chemically identical dyes differing only in size—DiIC(2), DiIC(6), and DiIC(14) in *n*-alcohols—together with the authors of ref 45. In this work both absorption recovery and fluorescence data were used. According to these results, which will be published in a forthcoming paper (*J. Chem. Phys.*), the G–W correction brings all data points of DiIC(2) into a very smooth curve with very little scatter. When Kramers' function is fitted to these results, still slight but evident undershooting of the reduced rates is observed at high values of friction. The correction does not bring much improvement for the larger dye molecules, for which more or less linear isoviscosity plots are obtained. These results agree nicely with the main conclusions suggested by Ben-Amotz et al.,[22,52] in their two recent studies on rotational friction in solution: hydrodynamics will describe rotational motion in solution when solute molecules are large in size as compared to solvent molecules.

We calculated the G–W rotational correlation times for our fluorescence data as well. The details of these calculations will be given in our fourthcoming paper. The procedure was considered worth while, after realizing that the nonradiative rates of DiIC(2) plotted as a function of η/T produced linear but solvent dependent correlations (Figure 8). Both DSK and G–W models produce rotation relaxation times for a particular solute in solution, which are dependent on the relative volume ratio of the two and accordingly are typical of solvent environment. To visualize the effects of volume correction, the observed reduced rates were first

(50) Dote, J. L.; Kivelson, D.; Schwartz, R. N. *J. Phys. Chem.* **1981**, *85*, 2169.
(51) Gierer, A.; Wirtz, K. *Z. Naturforsch.* **1953**, *8a*, 532.

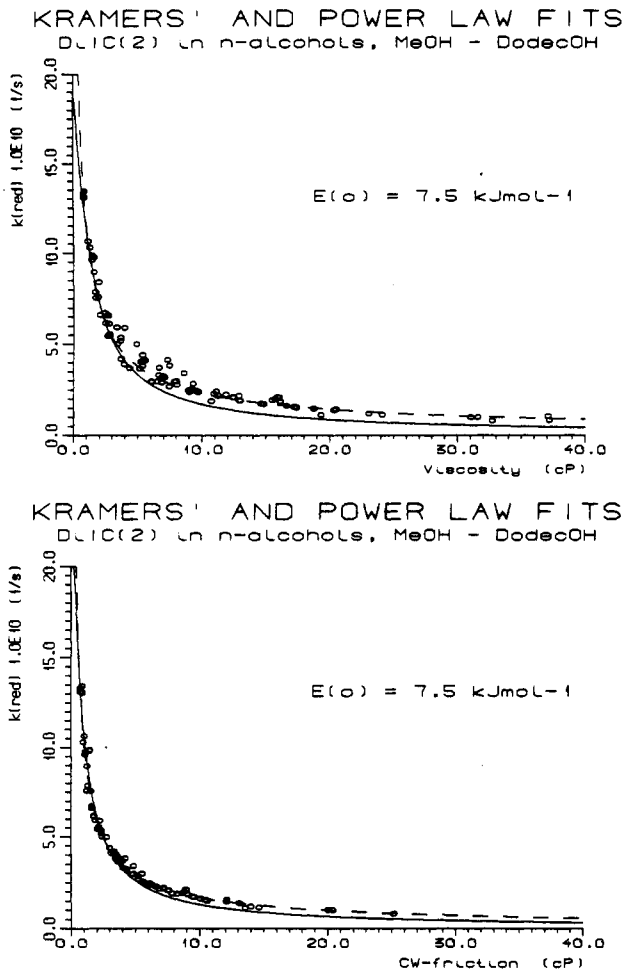

Figure 9. Fit of Kramers' equation (solid line) and the power law equation (dashed line) by using (a, top) hydrodynamic friction (b, bottom) G–W friction with the reduced rates. For fitting parameters see text.

fitted by using the hydrodynamic Kramers' model and a constant barrier height of 7.5 kJ mol^{-1}. The results are shown in Figure 9a. Kramers' constants $A = 2.24 \times 10^{11}$ Hz and $B = 1.62$ cP were obtained. Calculating theoretical rotational correlation times and the corresponding values of friction by using the G–W model, the observed reduced rate constants were then again fitted to Kramers' equation (Figure 9b). Kramers' constants of $A = 2.60 \times 10^{11}$ Hz and $B = 1.01$ cP were obtained. Figure 9b clearly shows that the volume correction brings the data points onto a smooth curve, removing the scatter of the data points observed in the hydrodynamic Kramers' plot (Figure 9a). The correction has the effect of slightly increasing the Kramers' frequency at the initial potential well and decreasing the frequency at the barrier top, allowing for faster rates in long-chain solutions. Correction does not remove slight undershooting of Kramers' rates at high values of friction. From Figure 9 it is concluded that the relative volume ratio is an important factor in determining the microscopic friction of isomerization reactions in solutions, where the size of the solute molecule becomes equal or smaller than that of the solvent molecule.

Effective Viscosity. An alternative way of accounting for the nonlinearity of the isoviscosity plots is to find those temperatures and corresponding "effective" viscosities that would make the observed nonradiative rates of long-chain alcohols fall on the lines extrapolated from short-chain solvent data (see Figure 4b). A constant barrier height of 7.5 kJ mol^{-1} was assumed. The "effective viscosities" of the reaction obtained in this way are shown in Figure 10. Besides butanol the effective viscosities seem to be lower than the corresponding hydrodynamic viscosity. "Effective viscosities" and a constant barrier of 7.5 kJ mol^{-1} of the reaction were used to produce a new Kramers' fit for datapoints from all solutions (Figure 11a). The plot shows almost similar

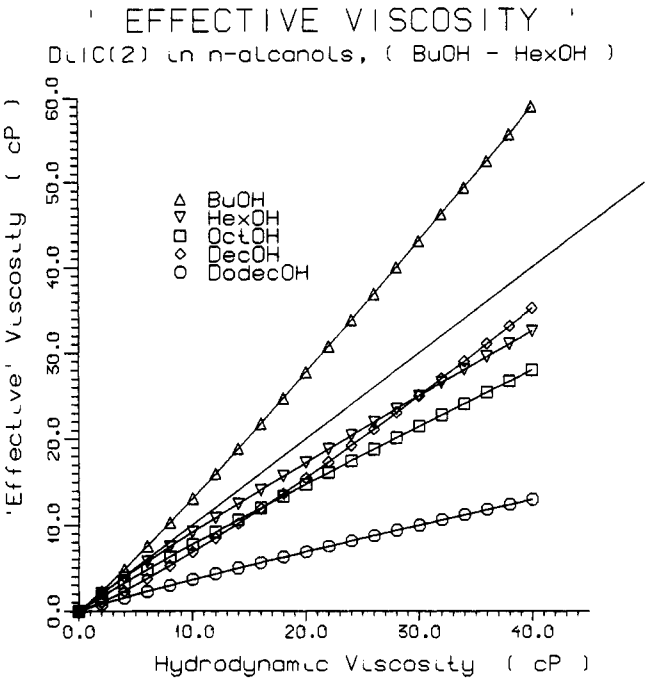

Figure 10. "Effective" viscosities obtained by assuming a constant barrier height of 7.5 kJ mol^{-1} for the reaction in all solvents studied. For details of obtaining the effective viscosities see text. The line without symbols represents one-to-one correspondence to the hydrodynamic viscosity.

scatter of the observed rates as the hydrodynamic Kramers' plot (Figure 9a). Kramers' parameters obtained for short-chain alcohols and those obtained after viscosity correction compare nicely with each other; in the former case we have $A = 2.10 \times 10^{11}$ 1/s and $B = 1.65$ cP and in the latter case $A = 2.18 \times 10^{11}$ 1/s and $B = 1.58$ cP. The "effective viscosity" correction does bring the observed data points roughly onto a single Kramers' curve, the shape of which is very similar to that obtained for the short-chain solutions in the hydrodynamic limit. Slight undershooting at high viscosities is still observed.

It is interesting to compare our "effective viscosities" to the theoretical G–W rotational friction of DiIC(2) in *n*-alcohols. Both can be compared to the hydrodynamic viscosity. From the "effective viscosity" plots at 20 cP one obtains correction factors 1.4, 0.63, 0.55, 0.57, and 0.26 for butanol, hexanol, octanol, decanol, and dodecanol, respectively. The corresponding factors from the G–W model are 0.77, 0.70, 0.64, 0.61, and 0.56. The agreement between the three intermediate factors is at least fair. Most of the scatter of the experimental rates in Figure 11a is from butanol and dodecanol data.

Reduced Rates at High Values of Friction. The diffusion limit of Kramers' theory at high values of friction predicts the reduced rates of isomerizing being inversely proportional to friction (eq 4). At this limit velocity correlation time of the reaction coordinate becomes short as compared to time scales of free motion on the potential surface. It has been shown that for low barriers or for zero barriers Smoluchowski behavior is valid.[7,45] For higher barriers deviations from Kramers' and from Smoluchowski behaviors are observed. The reaction becomes increasingly barrier controlled. The time spent in the barrier region becomes short and the medium response has to take place during a short time to be effective. Intuitively one can predict that the reaction does not feel the full respose from the solvent environment. "Too fast" reduced rates or "too low" friction of the reaction are observed.

To study the undershooting of the reduced rates in Kramers' picture at high values of friction, we assume Smoluchowski type dependence of the observed rates on friction. We further assume that small deviations from simple hydrodynams can be accounted for by using a boundary condition:

$$\xi_i = D_i(\eta/\eta_0)^{\alpha_i} \qquad (5)$$

where D_i has the dimension of friction, exponent α is a constant ($0 < \alpha_i \leq 1$), and η_0 is the reference shear viscosity. When α_i

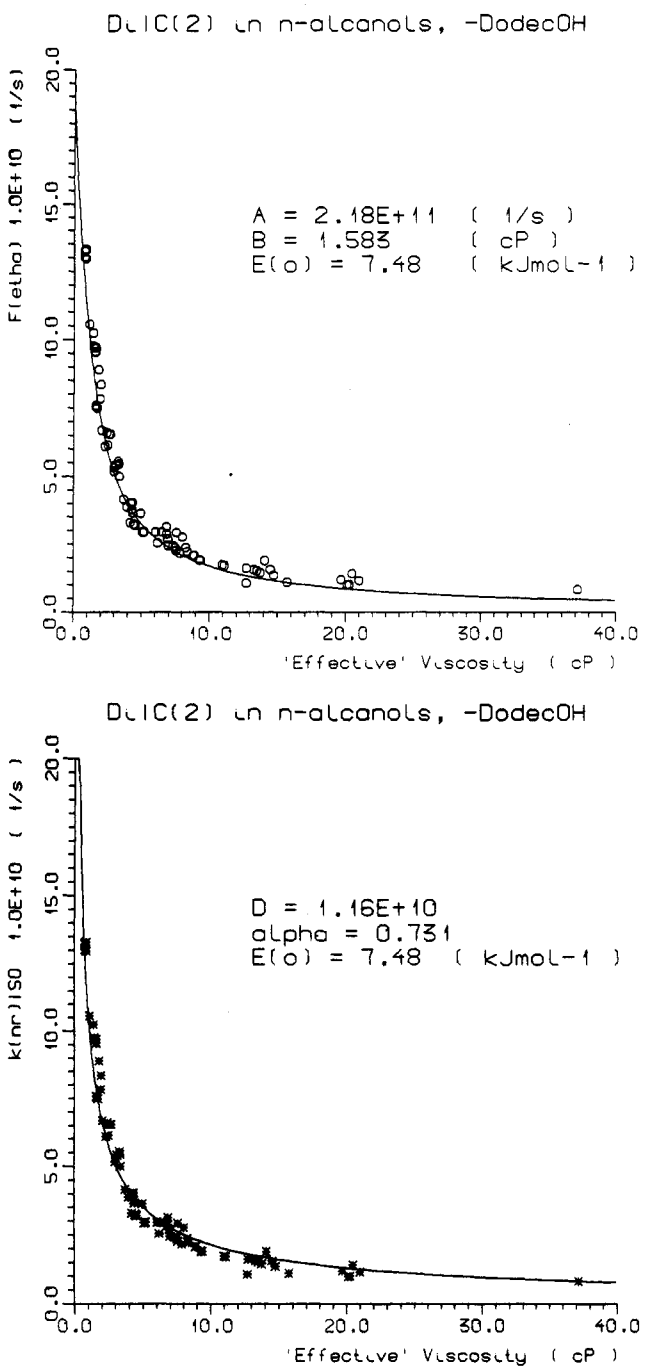

Figure 11. Fit with the reduced rates using 'effective viscosities': (a, top) Kramers' equation; (b, bottom) power law equation. Results for all solutions except dodecanol are included.

is unity, the hydrodynamic boundary conditions are met. If α_i is less than unity, the friction becomes smaller than the corresponding shear viscosity of the solution. By inserting eq 8 into eq 4 and rearranging, we get

$$\ln (k^i_{nr}) = \alpha_i \ln D'_i - \alpha_i \ln \eta - E_0/kT \qquad (6)$$

where $D'_i = \omega_a\omega_b\eta_0/2\pi D_i$. Assuming that α_i does not vary much from solvent to solvent, eq 9 predicts linear and parallel $\ln (k^i_{nr})$ versus $1/T$ plots at constant viscosities, the behavior we see in short-chain solutions (Figure 4b). Linear isoviscosity plots have been observed in most of the earlier studies of isomerizing reactions.[4,7,45] Equation 9 implies also that at constant temperatures the logarithm of the nonradiative is a linear function of logarithm of viscosity. These plots for DiIC(2) of *n*-alcohols at four temperatures are shown in Figure 12. Nonlinear behavior becomes apparent at high temperatures (at +80 °C). Constant α seems to be slightly temperature dependent (at 80.0 °C α = 0.63, while at −40.0 °C α = 0.74), the average value being 0.69.

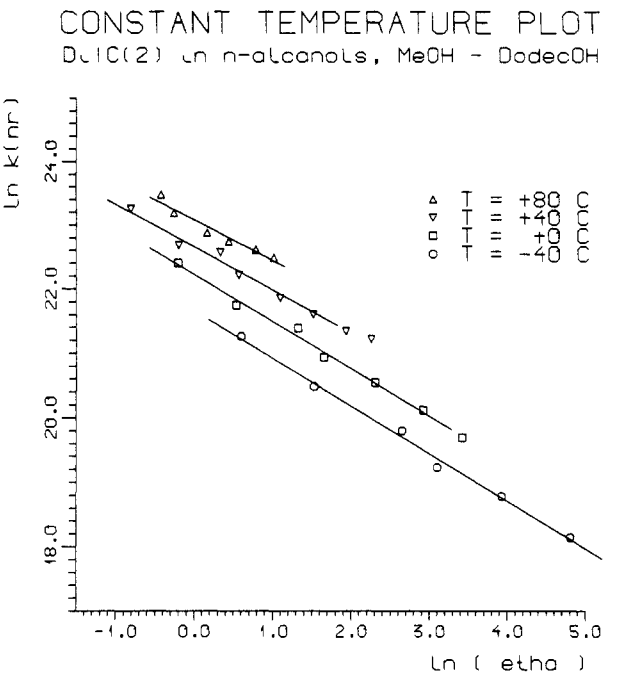

Figure 12. Logarithmic plot of the nonradiative rates as a function of viscosity at constant temperatures according to eq 6. The average of slopes gives α = 0.69.

Assuming exponential temperature dependence of η in each solvent (as in Table II), we get

$$\ln (k^i_{nr}) = \ln D''_i/\eta_{0i}^{\alpha i} - (1/kT)(E_0 + \alpha_i E_{\eta i}) \qquad (7)$$

where activation energy takes the form $E_{\alpha i} = E_0 + \alpha_i E_{\eta i}$. The constant α_i may vary from solvent to solvent. Equation 10 predicts linear Arrhenius behavior in each solvent. This has been verified in most earlier studies. In our approximation the parameter α_i scales the viscosity-dependent part of the activation energy. At the Smoluchkowski limit, when α_i is unity, $E_\alpha = E_0 + E_\eta$. For most isomerization reactions $E_\alpha > E_0 + E_\eta$[7,45] and the discrepancy grows as the barrier height becomes large relative to E_η. If α is less than unity, as it usually is, then eq 10 gives rates higher than one would expect from the high-viscosity limit of Kramers' equation.

Since $E_{\eta i}$ and $E_{\alpha i}$ are known quantities, E_0 and α_i can be evaluated from temperature dependencies of nonradiative rates in chemically similar solvents. In this case we have data for eight *n*-alcohol solutions. Making an isoviscosity plot serves as a good averaging method of E_0. For solutions from methanol to hexanol we get E_0 = 7.5 kJ mol^{-1}. The equation $E_{\alpha i} = E_0 + \alpha_i E_{\eta i}$ was then used to study whether α_i is independent of the solvent. To a very good approximation this is the case, and we get an average value of α = 0.69 (0.04) in all solvents. This value compares nicely with the average value obtained from constant temperature plots by using eq 6.

Equation 6 can be transformed into

$$k_{red} = k_{nr}e^{E_0/kT} = D/\eta^\alpha \qquad (8)$$

Similar equation can be derived on totally different grounds by considering the rate of molecular rearrangement in the presence of solvent[53] and by relating viscosity to the free volume of the solvent.[39,40]

We have used eq 8 to fit our kinetic data along with the Kramers' plots (Figures 6, 7, 9, and 11). A common feature in all these plots is that eq 8 produces better fits than is obtained from hydrodynamic Kramers' theory at high values of friction. We suggest that the parameter α accounts for apparently low values of friction and for faster observed rates in the high friction

(52) Ben-Amotz, D.; Scott, T. W. *J. Chem. Phys.* **1987**, *87*, 3739; Ben-Amotz, D.; Drake, J. M. **1988**, *89*, 1019.
(53) Gegiou, D.; Muzkat, K. A.; Fischer, E. *J. Am. Chem. Soc.* **1968**, *90*, 12.

end. The physical underlying reason for the observed behavior may be the slower response of the solvent on the reaction coordinate under these conditions.[32] The nonlinearity of the isoviscosity plots observed for long-chain alcohol solutions seems to arise from another effect. Removing the nonlinearity from isoviscosity plots by using "effective viscosities" does not improve the Kramers' fit at high values of friction (compare Figures 6 and 9). Our results do not suggest a connection of α to the molecular properties of the solution. However, we prefer a relation to frictional properties of the reaction rather than relative volume effects in solution.[22,39,40,51]

Fitting all data points using hydrodynamic and "effective viscosities" (see Figures 9a and 11) to eq 8 gives $D = 1.15 \times 10^{11}$ 1/s and $\alpha = 0.66$ in the former and $D = 1.16 \times 10^{11}$ 1/s and $\alpha = 0.73$ in the latter case, respectively. The α's obtained from the above fits are fairly close to the average value 0.69 obtained from eq 6 at constant temperatures (Figure 12). The corresponding constants from G-W corrected data are $D = 1.03 \times 10^{11}$ 1/s and $\alpha = 0.78$.

Extended Kramers' Theory. Recently, Robinson et al.[35] have suggested an empirical equation to describe nonradiative kinetics of seven isomerizing dyes in *n*-alkanols. We have used the equation to model the isomerization kinetics of DiIC(2) dye. Reasonable fits to our data were obtained for solutions from methanol to hexanol. Constant A_3 became an extremely sensitive fitting parameter and reached an unexpected value of less than unity for the best fits. For the higher alcohols fits were very bad. Inserting the reduced rates observed at 1 and 10 cP into "extended Kramers" equation and using a value of 1.01 for A_3 gave a negative value of parameter A_2. Since A_2 is related to the transition-state rate, a negative value is not acceptable. The extended Kramers' equation seems to work only in cases where not too strong viscosity dependence of the reduced rates is observed.

Conclusions

We have studied the isomerization reaction of the cyanine dye DiIC(2) in eight *n*-alcohols and at several temperatures. Fluorescence lifetime measurements were used to extract the nonradiative rates of the reaction. The observed nonlinearities of the isoviscosity plots were studied by assuming a viscosity dependence of the barrier height. The method produced a nice Kramers' fit of the observed rates, but unrealistic Kramers' parameters were obtained. Accordingly, frictional rather that barrier-dependent properties of the isomerization reaction were considered to give rise to nonlinearities observed for the isoviscosity plots in long-chain alcohol solutions.

Isomerization of DiIC(2) involves a motion that is very close to molecular rotation. Using the Stokes-Einstein model for rotational relaxation produces solvent-dependent correlations. To account for solvent dependence Gierer-Wirth type rotation, correlation times can be used to estimate microscopic friction in solution. Correction brings the experimentally observed rates onto a smooth curve. It may be concluded then that the relative volume ratio of the solute and solvent is an important factor in determining the microscopic friction in solutions, where solute size becomes equal to or smaller than that of the solvent. Kramers' fit of the volume corrected data still produces too slow reduced rates at high values of friction. By calculation of "effective viscosities" from the curved region of the isoviscosity plots, an estimate of microscopic friction was obtained. These values of friction of the reaction compare qualitatively to the theoretice values of friction obtained from volume corrected rotational correlation times. Using "effective viscosities" and the reduced rates from all solutions gave similar Kramers' parameters as was obtained from data measured in smaller *n*-alcohols.

A near Smoluchowski type equation allows adequate fitting of the reduced rates at high values of friction. In this limit we believe that frequency-dependent friction plays an important role in controlling the isomerization reaction. At low temperatures and high viscosities the solvent response to the reaction coordinate becomes slow even for moderately low barriers.

Acknowledgment. The Academy of Finland is gratefully acknowledged for financial support. We are indebted to Drs. Villy Sunström and Thomas Gillbro for suggesting this study and for several critical discussions during the course of this work. We also want to thank Emmet OY, Finland, for providing us with the PAR OMA system for a short time to record the fluorescence spectra reported in this study.

Registry No. DiIC(2), 14696-39-0.

Chemiluminescence in the Reactions Mn + O_2, NO_2, CO_2, and SO_2

Martin R. Levy

Department of Chemical and Life Sciences, Newcastle Polytechnic, Ellison Building, Ellison Place, Newcastle upon Tyne NE1 8ST, U.K. *(Received: July 17, 1990; In Final Form: May 24, 1991)*

A laser-ablated pulsed beam of Mn atoms has been employed to determine the translational energy dependence of the chemiluminescent processes $Mn(a^6S,a^6D_J,...) + RO \rightarrow MnO^*(A^6\Sigma^+) + R$, where R = O, NO, CO, and SO. Analysis of the excitation functions by microcanonical transition-state theory indicates that only a very few Mn states contribute significantly—most probably a^6D_J, a^4D_J, and perhaps (in the O_2 case only) z^8P_J. With the exception of $Mn^*(a^4D_J) + O_2$ and CO_2, the results are consistent with simple adiabatic state correlations. All a^6D_J-assigned reactions appear to proceed through a potential well, with a barrier in the exit channel; but, as collision energy increases, most, if not all, of the excitation functions change to the simple line-of-centers form, indicating that the well no longer influences the transition-state dynamics. Depletion in the chemiluminescence at higher energies still is attributed to "recrossing".

Introduction

A major problem inhibiting investigation of transition-metal atom reaction dynamics has been the high refractivity of the elements. However, as demonstrated in a previous paper,[1] pulsed laser ablation of a solid metal target provides a means of overcoming this difficulty. The technique allows generation of a pulsed beam of metal atoms, of wide velocity range and containing a number of metastable states in addition to the ground state. Excitation functions for luminescent reactions and energy-transfer processes can be obtained by allowing the pulsed beam to interact with a low pressure of a suitable reactant gas and observing the

(1) Levy, M. R. *J. Phys. Chem.* **1989**, *93*, 5195.

0022-3654/91/2095-8491$02.50/0